Omni Applied Science

Create • Curate • Educate

Integrated Probabilistic Modeling of Sea Ice, Metocean Conditions, and Vessel Operability for Estimating Weather Windows in Arctic Offshore Drilling

Christopher J. Jablonowski

Report 25-6

September 1, 2025

Acknowledgments

The author thanks John Henley, Robert Raye, Mark Newell, Jason Smith, Michael Vogel, Caspar Heyl, Job Baar, Adam Scheidler, Justin Barrow, and Josiah McVicar.

All errors and omissions remain the responsibility of the author.

Related Publication and Version Notice

A peer-reviewed version of this report was published as:

> Jablonowski, C.J. 2026. Integrated Probabilistic Modeling of Sea Ice, Metocean Conditions, and Vessel Operability for Estimating Weather Windows in Arctic Offshore Drilling. *ASME Journal of Offshore Mechanics and Arctic Engineering*, Vol. 148(5): 051602.

This report is an earlier pre-publication manuscript that may differ in content from the published version. The final version of record is available from the publisher. The Creative Commons license applies only to this report and does not apply to the journal-published article.

Suggested Citation of This Report

> Jablonowski, C.J. *Integrated Probabilistic Modeling of Sea Ice, Metocean Conditions, and Vessel Operability for Estimating Weather Windows in Arctic Offshore Drilling*. Report 25-6. Houston, TX: Omni Applied Science, 2025.

About Omni

Omni Applied Science is an operating company that manages a diverse portfolio of scientific, engineering, economic, and management science business units.

We partner with clients to frame and define their unique requirements, and assemble bespoke teams from our global network of expert consultants and academics to deliver specialized support and solutions. Our delivery model ensures that technical expertise is deployed precisely and efficiently on behalf of our clients, maximizing value through actionable insights.

We conduct research with clients and also perform independent research in support of our activities. This report presents research completed to support internal analysis, client advisory work, and broader technical and economic understanding.

Executive Summary

This paper presents a probabilistic Monte Carlo simulation workflow that integrates sea ice dynamics, seastate conditions, and vessel operability to estimate weather windows for Arctic offshore drilling. The analysis also demonstrates how estimates of the weather window can be used to develop probabilistic cost and schedule estimates for drilling activities. Using 12 years of sea ice observations and 29 years of wave data for a Chukchi Sea drilling site, a first-order, time-inhomogeneous Markov chain is specified to estimate week-to-week site availability under open-water/sea-ice-free conditions (<10% ice concentration). Drilling rig operability is estimated based on joint wave direction–height distributions, drilling vessel flex-joint angle limits, and operator response (rig rotation) when operating limits are exceeded. A Monte Carlo simulation yields a probability distribution of the duration of the July–November operating season. When integrated with drilling activity cost and schedule information, the framework provides a quantitative foundation to develop risk-based cost and schedule estimates to support project planning and decision-making at various levels, from portfolio management and asset evaluation to detailed execution planning.

Contents

INTRODUCTION

The United States (US) Arctic offshore is a potentially resource-rich oil and gas basin. For example, the Bureau of Ocean Energy and Management (BOEM) of the US Department of the Interior estimates that the Chukchi Sea Planning Area offshore of Alaska may hold 15.4 billion barrels of technically recoverable oil and 76.8 trillion cubic feet of technically recoverable natural gas. This is second only to the Central Gulf of Mexico in terms of offshore resource potential in the US. The Beaufort Sea also has significant resource potential estimated by the BOEM at 8.9 billion barrels of oil and 27.7 trillion cubic feet of natural gas [1]. These regions are depicted in Fig. 1 and are the immediate areas of interest for this analysis. The entire arctic offshore region is estimated to hold 90 billion barrels of technically recoverable oil and 1,670 trillion cubic feet of technically recoverable natural gas [2].

Based on geophysical and geological assessments, exploration drilling programs are designed to test and appraise potential oil and gas reservoirs. If warranted, development projects are initiated to produce the resources. These projects require wells to be drilled and production facilities to be constructed (e.g., flowlines, structures, processing facilities). Cost and schedule estimates for all these components are core inputs to numerous processes and computations, for example: economic analysis (net present value and project ranking), project selection and portfolio management, and execution planning.

The accuracy of cost and schedule estimates is crucial. Overestimates may cause a project to be unduly de-prioritized or lead to an unwarranted exit decision. Underestimates have the opposite effects and promote undeserving projects that ultimately fail to meet targets, destroy value, and cause reputational damage. While all capital projects must account for some uncertainty in cost and schedule estimates, projects in the Arctic offshore pose unique challenges. For example, to conduct well construction operations in the Arctic offshore, operators mobilize significant resources and incur irreversible fixed costs long before the weather conditions are known. In cases where the presence of ice or severe weather prevents completion of project scope within a season, the operator will have to return in a future year (or years), once again incurring large mobilization costs. There also may be stand-by costs incurred in the off-season to maintain assets or to guarantee access to supplier resources in future years. Because capital costs for large oil and gas projects often are measured in billions of dollars, the importance of accurate cost and schedule estimates for economic analysis, planning, and decision-making is self-evident.

With respect to cost and schedule estimates, the primary uncertainties that must be addressed in Arctic projects are metocean conditions, specifically sea ice dynamics and seastate conditions. When these conditions deteriorate, operations may be suspended because of equipment operating limits, to protect workers, or to mitigate damage to equipment, other assets, or the environment. In extreme cases, not only will operations be suspended, the entire work site may be temporarily abandoned. The cost and schedule impacts of such disruptions include the time and costs of suspension and re-activation activities, standby costs for labor and equipment, and decreased productivity. Examples of the analysis of metocean risk and the impacts on cost and schedule can be found in Maes et al., Li et al., Rahman et al., and Towe et al. [3-6].

Therefore, estimation of a *weather window*—a period of time when metocean conditions permit normal operations without the aforementioned risks and costs—is a critical step in the cost and schedule estimating process, and the central purpose of the present analysis. Numerous methods have been developed and applied to estimate weather windows and to model the associated practical impacts. For example, Heo et al. [7] specify a Markov chain simulation to generate synthetic weather conditions, and specify an algorithm to simulate decision-making to identify optimal operational policies. Walker et al. [8] conduct statistical analysis and specify cumulative distribution functions to estimate the likelihood and duration of severe weather events that would affect operability. Yang et al. [9] use spectral wave models to simulate wave height and evaluate weather windows to estimate the efficiency of construction operations.

This work develops an integrated probabilistic framework using historical metocean data to estimate site-specific weather windows for Arctic drilling. The workflow incorporates (i) sea ice dynamics via a first-order time-inhomogeneous Markov chain, (ii) seastate operability via joint wave direction–height distributions and vessel-specific response limits, and (iii) operational decision rules. The resulting distribution of total operating days is then combined with a probabilistic drilling schedule estimate to estimate a distribution of the number of seasons required to complete a given scope of work. Simulation is appropriate because forecasts of the metocean conditions—especially for many years in advance—are available only as probability distributions. Early discussion of Monte Carlo (or probabilistic) simulation in engineering and economics can be found in Eubank et al. [10]. Initial applications were presented by Cardello et al., White, and Klausner [11-13], with more recent examples found in Farr et al., Leheta et al., and de Werk et al. [14-16]. The present analysis integrates sea ice dynamics, seastate conditions, vessel impacts, and operational responses in a probabilistic framework. In addition, the simulation includes uncertainty in the activities themselves. The framework is an extension of earlier applications of cost and schedule modeling in the oil and gas literature described in Zoller et al., Williamson et al., Akins et al., Hariharan et al., Kaiser and Pulsipher, Adams et al., and Jablonowski et al. [17-23].

The main contribution of this work is a practical and novel framework that models the joint effects of sea ice dynamics, seastate conditions, and operator responses to estimate the seasonal weather window for an offshore drilling vessel. We also demonstrate how to combine this information with schedule estimates to develop a fully integrated probabilistic estimate of drilling cost and schedule. The output provides the quantitative foundation required for accurate economic analysis and execution planning in capital-intensive Arctic projects.

The remainder of the paper is organized as follows. Section 2 specifies a model to predict site availability based on sea ice dynamics. Section 3 develops the statistics regarding seastate conditions that are required for simulation. Section 4 describes the interaction between seastate conditions and the drilling vessel, and integrates operational rules to specify a preliminary probabilistic simulation for the distribution of rig operating days. Section 5 combines the sea ice, seastate, and vessel information to specify the full probabilistic simulation of total operating days, or weather window. Section 6 provides a demonstration of how the probabilistic simulation can be combined with a drilling schedule estimate to estimate a distribution for the number of seasons required to complete a defined scope of work. Section 7 concludes.

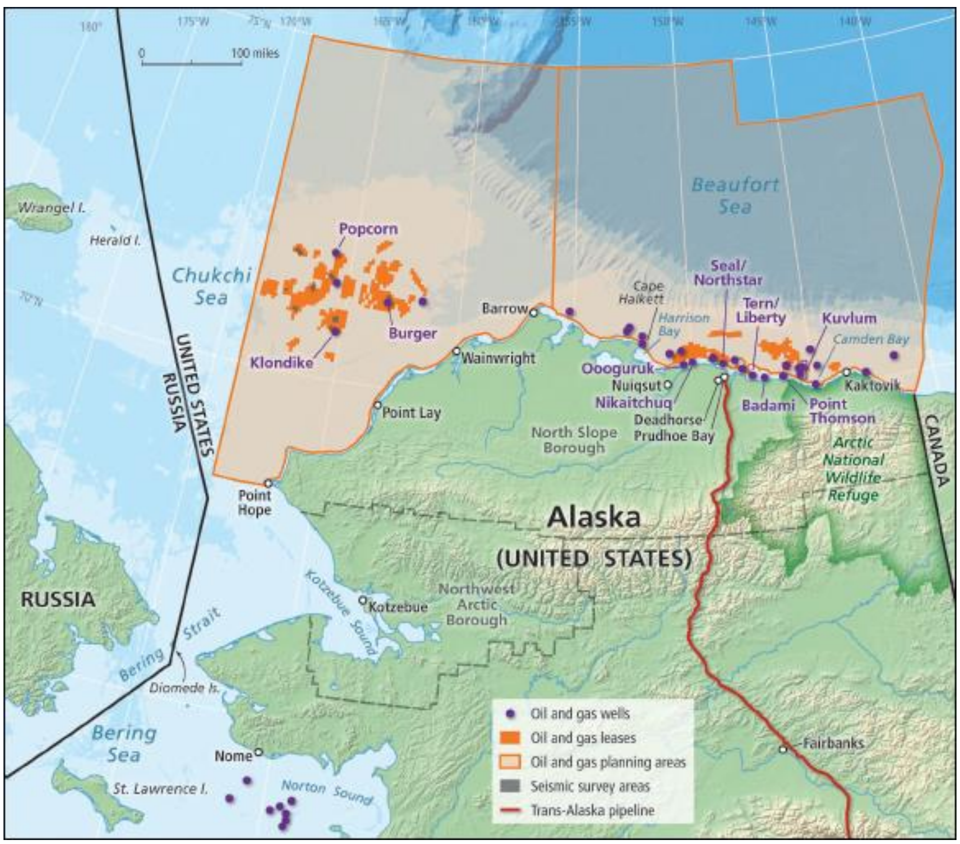

Figure 1. Oil and gas planning areas in the Chukchi and Beaufort Seas [24]

SEA ICE DYNAMICS

Sea ice concentration is a critical factor affecting offshore oil and gas operations in the Arctic. When sea ice concentration is too large, drilling and support activities (e.g., marine logistics) may be partially suspended, fully shut-down, or the drilling rig may be forced off location [5]. Because of these and related impacts, empirical analysis of sea ice formation and melting—and their interseasonal variability—have been studied extensively in the research literature, see Pan et al., Steele et al., Peng et al., and Bliss et al. for recent examples [25-28].

Statistical analysis of sea ice concentration was conducted for the proposed project site in the Chukchi Sea, inclusive of a 15-mile radius buffer zone. The primary data source is the US National Ice Center, and it is supplemented with related resources and tools (e.g. MODIS satellite imagery).[1] In this study, drilling operations are considered fully *available* under Open Water (<10% sea ice concentration) or Sea Ice Free (OW/SIF) conditions. This criterion was selected to represent a reference case of freely navigable conditions where it can be assumed that ice-management measures are not necessary. This strict condition could be relaxed if icebreakers and ice-management vessels were deployed as described in Eik [29-30] and Teigen et al. [31]. The economic viability of such measures depends on the cost-benefit tradeoff between the additional operating expense of an ice-management fleet and the expected increase in the length of the weather window and the associated cost savings. Because the present work focuses on development of an integrated probabilistic framework, the analysis of ice-management alternatives is reserved for future study. Also, we acknowledge that long-term trends and most projections indicate increasing retreat of Arctic summer sea ice, potentially yielding longer weather windows in the Chukchi Sea as reported in Meier et al. [32]. If such sea ice projections are incorporated into estimates, more projects would be assessed as economically viable and successfully compete for funding. And if the projections are accurate, resources would be developed more rapidly. However, the current workflow is based on stationary historical statistics, and investigation of alternate scenarios is not included here.

The analysis uses 12 years of detailed observational data, and evaluates five months in each year including July through November.[2] To support subsequent simulations, sea ice concentration observations were divided into four approximately equal time periods within each month—referred to as *weeks* hereafter. We define a binary

[1] MODIS - Moderate Resolution Imaging Spectroradiometer.

[2] While the sample exhibits some availability in June, it was decided to conduct detailed analysis from July to November because of operational and commercial factors related to logistics and contracting, and other constraints.

variable, ice_{tw}, that takes on a value of 1 when drilling operations are available in year t ($t = 1 \ldots 12$) and week w ($w = 1 \ldots 20$), and 0 otherwise.

There are numerous options for specifying the simulation of sea ice concentration and the respective availability of drilling operations. One could evaluate the observational data and compute the mean and standard deviation of the available weeks per year and simulate based on those statistics. However, this approach is inadequate for cost and schedule estimating because it obscures month-specific differences in variability and the associated interaction between availability and seastate conditions.

A more detailed approach can be specified by estimating the marginal probability of availability for each week, defined as $\hat{c}_w = \Pr(ice_w = 1) = \frac{1}{12}\sum_{t=1}^{12} ice_{tw}$, and sample availability using these estimates. This approach assumes statistical independence of the same week between years, but more importantly, statistical independence among all weeks within the same year. While the former assumption is reasonable given the purposes of this analysis, the latter is probably not because sea ice conditions exhibit strong intraseasonal temporal relationships [27-28, 33].

To explicitly address the temporal dependence in sea ice conditions, a second approach was specified to model week-to-week availability. We specified a simple intraseasonal, first-order, time-inhomogeneous Markov chain model of week-to-week availability, expressed as: $\hat{c}_i^{(w)} = \Pr\big(ice_{tw} = 1 \mid ice_{t(w-1)} = i\big)$, for $i \in \{0,1\}$. The first week of July (July-1) was seeded based on its estimated marginal probability of availability, $\hat{c}_1$.[3] Week-specific transition probabilities, $\hat{c}_i^{(w)}$, were estimated based on the observed week-to-week conditional frequencies. It is probable that the true correlation structure is more complex and a simple Markov model will be misspecified (e.g. correlation between non-adjacent weeks, interseasonal correlations, non-Markovian dynamics, and/or other meteorological or oceanographic relationships). Examples of more elaborate specifications of Markov models of sea ice dynamics are found in Chen and Yuan, Yuan et al., and Wang et al. [35-37]. But using the limited sample size (12 years) to specify a complex correlation structure creates a significant risk of misspecification and/or overparameterization [7]. Given the accuracy-misspecification tradeoffs, it was decided that a simple Markov model would be sufficient for the purposes of this analysis.

[3] Because of the importance of initial conditions (see Msadek et al. [34]), and the somewhat small sample available in this study, a potential extension of this approach could specify the initial marginal probability of availability as a random variable itself. Such an analysis also could be employed for all the marginal and transition probabilities to account for the potential bias deriving from the limited sample.

The first part of the probabilistic simulation regarding availability is specified using both statistical approaches and a sample size of 2,500. Each sample represents a potential sequence of week-to-week availability for the July to November season. In the first approach, weeks are assumed to be statistically independent, and ice_w is sampled using the estimated marginal probability for each week. In the second approach using the Markov model, ice_w is sampled (seeded) for the first week of July as previously described, and the transition probabilities are used to sample ice_w for subsequent weeks. The seasonal availability is the sum of available weeks, $ice_t^* = \sum_{w=1}^{20} ice_w^*$. Statistics for the observational data and representative results of the simulated probability distributions of seasonal availability are reported in Table 1.

Table 1. Seasonal Availability Statistics for the Observational Data and Simulated Probability Distributions (weeks)

Statistical Property	Observational Data	Independent Weeks	Markov Model
Minimum	3.0	5.0	1.0
P10	6.0	9.0	6.0
P25	9.0	10.0	9.0
Mean	10.8	10.8	10.7
P75	13.3	12.0	13.0
P90	14.0	13.0	14.0
Maximum	18.0	16.0	18.0
Standard Deviation	4.1	1.6	3.3
Sample Size	12	2500	2500

While both simulations adequately replicate the mean of the observational data, the independent-week model fails to replicate other important properties of the distribution which are important for cost and schedule estimating. Specifically, the distribution is significantly less dispersed than the observational data. This is an anticipated result because the independent sampling prevents long runs of (non)availability and thus fewer extreme sequences are observed. In contrast, the Markov chain model replicates the observational data well, and yields week-to-week availability sequences that are consistent with the observational data. It is noteworthy that the observational data contains seasons ranging from 15-90% availability, and we believe this aspect of the observations explains the Markov model's (good) variance-related performance. Also, the simulation results suggest that the simple Markov model is capturing a material component of the statistical dependence between weeks. The Markov model is used for all subsequent analysis.[4]

SEASTATE CONDITIONS

When drilling operations are available based on sea ice concentration, the seastate conditions become relevant. Wave direction and height are the most important factors because they impose significant loads on the drilling vessel and riser which are subject to operating limits. To develop the necessary inputs for simulation, statistical analysis of wave direction and height was conducted using 29 years of historical data. The analysis included a statistical evaluation of multiple wind-speed return periods, and specification of a 3 day decorrelation interval to avoid counting peaks from the same storm multiple times. The 1-minute, 10-meter wind speed was derived from the 1 hour values using the API/NPD[5] gust equations [38]. Regression analysis was used to estimate the associated significant wave height and wave peak period. The analytical issues associated with this type of historical analysis are described in the literature, for example see Guedes Soares and Carvalho, Fouques et al., Bitner-Gregersen et al., Martins Campos et al., Liao et al., and Yang et al. [39-44]. All statistics are estimated for the specified project location.

For each month of the operating season, we estimate a discrete joint probability distribution of wave direction $d_i\ (i = 1 \ldots 8)$ and significant wave height $h_k\ (k = 1 \ldots 25)$, defined as $\widehat{\mathrm{W}}(H_s = h_k, d = d_i)$ where $\sum_{k=1}^{25}\sum_{i=1}^{8}\widehat{\mathrm{W}}(H_s = h_k | d = d_i) = 1$. For example, the joint probability distribution for the month of July, reported as percentages, is provided in Table 2.

To organize the probability information for subsequent use in simulation, the probabilities for wave height for each wave direction are accumulated in 1 meter increment bins, $h_j^b\ (j = 1 \ldots 6)$. The estimates are then used to define a conditional probability distribution, $\widehat{w}^b(h^b|d) = \Pr(H_s^b = h^b | d = d_i)$, where $\sum_{b=1}^{6}\widehat{w}^b(h_b|d_i) = 1$. The result of this computation for the month of July is provided in Table 3. The marginal probability of wave direction, defined as $\widehat{w}_i^d = \Pr(d = d_i) = \sum_{k=1}^{25}\widehat{\mathrm{W}}(H_s = h_k | d = d_i)$, is also employed to support simulation

[4] We assessed convergence of the simulated distribution of seasonal availability for the sample size of 2,500 using 10 independent simulations. We estimated the 95% confidence interval for the simulated cumulative probability of availability at each week. For example, $P(ice_t^* \leq 12) = 0.657\ [0.648, 0.666]$. This was the widest observed confidence interval among all weeks, and this result was judged to be sufficiently precise for weather window estimation and cost and schedule estimating.

[5] American Petroleum Institute (API) and Norwegian Petroleum Directorate (NPD) (now part of the Norwegian Offshore Directorate).

computations. The marginal probability distribution for the month of July is provided in Table 4.

The historical seastate data and the associated probability information reflect various levels of sea ice concentration in the relevant months, whereas sea ice availability is assessed using a <10% sea ice concentration criterion as previously described. Thus, the two sets of information are somewhat mismatched. Also, there is some negative correlation between seastate conditions and sea ice concentration [45], and given <10% sea ice concentration, actual seastate conditions are expected to be somewhat less favorable than the historical seastate data. However, there is not sufficient information to specify a site-specific relationship between sea ice concentration and seastate conditions. Therefore, the weather windows estimated herein would be biased in an optimistic direction.

Table 2. Joint Probability Distribution of Wave Direction and Height (July) (%)

Wave Height Bin (m)	Wave Direction							
	1	2	3	4	5	6	7	8
	N	NE	E	SE	S	SW	W	NW
0.25	0.131	0.438	1.555	2.540	0.963	7.357	1.445	0.022
0.50	0.569	1.598	3.700	1.533	1.577	7.160	3.087	0.701
0.75	0.657	2.693	4.314	0.963	1.664	6.109	2.343	0.920
1.00	0.285	2.343	3.722	0.460	1.029	4.817	2.124	0.591
1.25	0.131	1.577	2.978	0.219	0.898	3.810	2.036	0.350
1.50	0.307	1.511	1.533	0.022	0.394	1.752	1.401	0.482
1.75	0.022	0.766	0.701	0.000	0.372	1.270	0.854	0.285
2.00	0.000	0.438	0.460	0.022	0.241	0.788	0.810	0.044
2.25	0.000	0.175	0.131	0.022	0.153	0.613	0.394	0.022
2.50	0.000	0.044	0.066	0.066	0.153	0.219	0.285	0.044
2.75	0.000	0.066	0.066	0.000	0.066	0.197	0.088	0.066
3.00	0.000	0.088	0.022	0.000	0.044	0.153	0.153	0.022
3.25	0.000	0.022	0.109	0.000	0.022	0.000	0.022	0.000
3.50	0.000	0.000	0.000	0.000	0.044	0.022	0.109	0.000
3.75	0.000	0.000	0.000	0.000	0.066	0.022	0.022	0.000
4.00	0.000	0.000	0.000	0.000	0.000	0.000	0.066	0.000
4.25	0.000	0.000	0.000	0.000	0.000	0.022	0.044	0.000
4.50	0.000	0.000	0.000	0.000	0.000	0.000	0.000	0.000
4.75	0.000	0.000	0.000	0.000	0.000	0.000	0.044	0.000
5.00	0.000	0.000	0.000	0.000	0.000	0.044	0.022	0.000
5.25	0.000	0.000	0.000	0.000	0.000	0.000	0.000	0.000
5.50	0.000	0.000	0.000	0.000	0.000	0.000	0.000	0.000
5.75	0.000	0.000	0.000	0.000	0.000	0.000	0.000	0.000
6.00	0.000	0.000	0.000	0.000	0.000	0.000	0.000	0.000
6.25	0.000	0.000	0.000	0.000	0.000	0.000	0.000	0.000

Table 3. Conditional Probability Distributions for Wave Height Given Wave Direction (July)

Wave Height Bin (m)	Wave Direction and Index							
	N	NE	E	SE	S	SW	W	NW
	1	2	3	4	5	6	7	8
1.00	0.781	0.601	0.687	0.940	0.681	0.741	0.586	0.630
2.00	0.219	0.365	0.293	0.045	0.248	0.222	0.332	0.327
3.00	0.000	0.032	0.015	0.015	0.054	0.034	0.060	0.043
4.00	0.000	0.002	0.006	0.000	0.017	0.001	0.014	0.000
5.00	0.000	0.000	0.000	0.000	0.000	0.002	0.007	0.000
6.00	0.000	0.000	0.000	0.000	0.000	0.000	0.000	0.000

Table 4. Marginal Probability Distribution of Wave Direction (July)

Wave Direction	Index	Marginal Probability
N	1	0.021
NE	2	0.118
E	3	0.194
SE	4	0.058
S	5	0.077
SW	6	0.344
W	7	0.153
NW	8	0.035

SEASTATE AND VESSEL INTERACTION

There are numerous examples in the literature that model the physical response of offshore structures to metocean loading. Donley and Spanos [46] analyze tension leg platforms, Winterstein and Torhaug, Winterstein et al., and Cassidy et al. [47-49] examine jackup drilling rigs, Karimirad and Moan [50] investigate spars, Ahmad and Datta, Sheehan et al., Ward et al., and McNeill et al. [51-54] study the response of marine risers. The present case involves a ship-shaped drilling vessel that can rotate around a moored turret located under the derrick.

When large lateral wave loads act on the drilling vessel, the vessel may be pushed off of center of the wellbore. When this occurs, large stresses are imposed on the lower flex-joint near the wellhead. To keep these stresses within allowable limits, the flex-joint angle is monitored, and if it becomes too large the risk is mitigated. The primary method of reducing the flex-joint angle is to rotate the vessel away from its default heading and into the direction of the waves to reduce the lateral wave loads. The rotation of the vessel requires suspension of most well operations and 12 hours to complete. Operations can resume after rotation in all but a small minority of cases. We assume that after the rig is rotated away from the default heading, it is rotated back to the default heading at an appropriate time (for example, based on short-term seastate forecast, rig operations, etc., but we do not model this level of operational fidelity). This re-rotation of the vessel also requires 12 hours, resulting in a total of one lost day per rotation event. The subject vessel is shown in Fig. 2 and a drawing of the marine riser is provided in Fig. 3.

Figure 2. Photograph of drilling vessel and service vessel

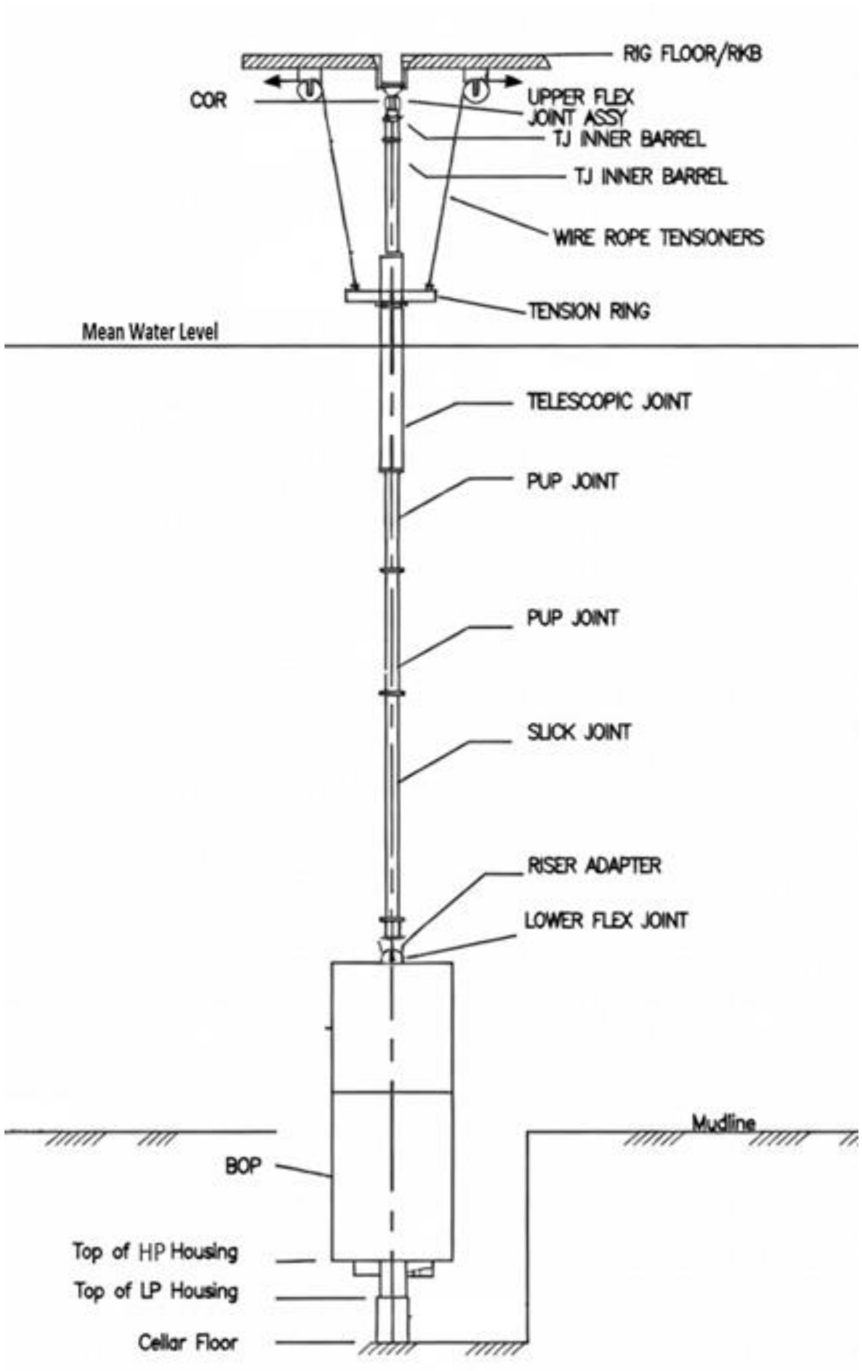

Figure 3. Marine riser showing location of lower flex-joint near the wellhead

A numerical model of this engineered system was specified and used to analyze the combined impact of wave direction, wave height, and vessel heading on the flex-joint angle. The position of the turret mooring lines was also accounted for. The design case assumes all anchor lines are undamaged, and the vessel heading is in between anchor lines.[6] Table 5 provides a summary of the relationship between flex-joint angle and (i) the difference between the wave direction and vessel heading, or encounter angle, and (ii) the wave height. As expected, the smallest flex-joint angles are observed when the encounter angle and wave height are small, and *vice versa*. To simplify the use of the numerical modeling results, fourth order polynomials were estimated for each wave height and are used as surrogates for the numerical model. The curve fits are provided in Fig. 4.

Table 5. Flex-Joint Angle (degrees) as a Function of the Encounter Angle and Wave Height

	Wave Height			
Encounter Angle (degrees)	1 m	2 m	3 m	4 m
0	0.2	0.4	0.9	1.8
5	0.2	0.4	0.9	1.9
10	0.2	0.4	1.0	2.0
15	0.2	0.5	1.2	2.4
20	0.2	0.6	1.5	3.0
25	0.3	0.8	2.0	3.8
30	0.4	1.1	2.5	4.5
35	0.4	1.4	3.1	5.1
40	0.5	1.6	3.7	5.6
45	0.6	1.9	4.1	6.1
50	0.7	2.0	4.3	6.4
70	1.0	2.7	5.4	8.4
90	1.3	3.1	6.2	9.7

[6] In cases where one or more mooring lines are damaged, operations are suspended until the line(s) are repaired. Analysis of this sub-case is not included here.

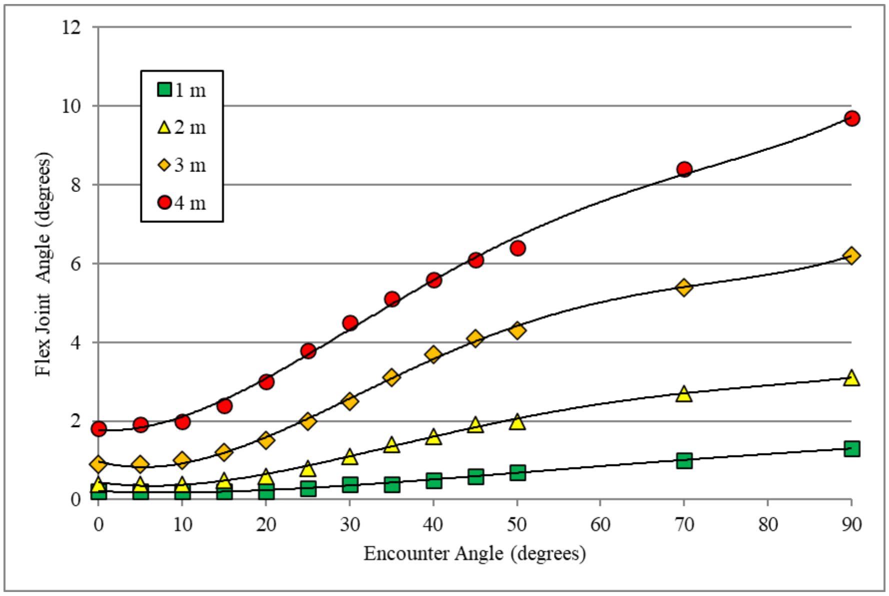

Figure 4. Curve fits for flex-joint angle (degrees) as a function of the encounter angle (1, 2, 3, and 4 m wave heights)

To combine seastate and vessel interaction information to estimate rig operability requires several steps. To accomplish this, a preliminary probabilistic simulation is specified where each sample represents a potential day in a specified month. The simulation proceeds as follows using a sample size of 2,500.

First, the wave direction is sampled based on the estimated marginal probability distribution for the specified month, and is denoted as d_i^*. For example, a partial result of 15 samples of wave direction for July is reported in column 1 of Table 6 (see Table 4 for the respective marginal distribution). Second, the wave height is sampled for each direction using the appropriate conditional probability distribution for the specified month, denoted as $h_j^{b^*}$ (see Table 3). Columns 2 to 9 in Table 6 report these results. Third, given the simulated wave direction in column 1, the appropriate wave height is selected from columns 2 to 9 and reported in column 10. This sequence of calculations generates samples of wave direction and height for the specified month (columns 1 and 10 in Table 6) in the format needed for input into the next step in the simulation.

Table 6. Simulated Wave Direction and Wave Height (July)

Sample #	Wave Direction d_i^*	Wave Height Bin (m)								Select: $h_j^{b^*}\vert d_i^*$
		$h_j^{b^*}\vert d_1^*$	$h_j^{b^*}\vert d_2^*$	$h_j^{b^*}\vert d_3^*$	$h_j^{b^*}\vert d_4^*$	$h_j^{b^*}\vert d_5^*$	$h_j^{b^*}\vert d_6^*$	$h_j^{b^*}\vert d_7^*$	$h_j^{b^*}\vert d_8^*$	
1	4	2	1	1	1	1	1	2	1	1
2	2	2	1	1	1	1	1	1	1	1
3	6	1	2	1	1	1	1	1	1	1
4	7	2	2	2	1	1	1	1	1	1
5	7	2	1	2	1	1	1	1	1	1
6	7	1	1	2	1	2	2	1	1	1
7	1	2	2	1	1	1	1	1	1	2
8	5	1	1	1	1	1	1	3	1	1
9	7	1	2	2	1	2	2	1	2	1
10	2	1	2	1	2	1	1	2	2	2
11	3	1	3	1	1	1	1	2	2	1
12	2	1	2	1	1	2	1	1	1	2
13	2	2	1	1	1	2	1	2	2	1
14	3	1	2	1	1	1	1	3	1	1
15	3	1	1	1	1	1	1	2	1	1

Finally, the surrogates in Fig. 4 are used to calculate the flex-joint angle as a function of the encounter angle and the wave height. The calculated flex-joint angle is compared to the user-specified threshold for risk mitigation. We define a variable to represent the drilling rig's operational status for each sample on any day in each month, OP_s $(s = 1 \dots 2500)$. If the angle is below the threshold, then it is a "rig operating day" and $OP_s = 1$. If the angle exceeds the threshold, then it is a "rig non-operating day," $OP_s = 0$, and the vessel is rotated into the direction of the waves as previously described. For each month, the estimated probability that $OP_s = 1$ is defined as $\hat{p}_s = \Pr(OP_s = 1) = \frac{1}{2500}\sum_{s=1}^{2500} OP_s$, and these probabilities are reported in Table 7.[7]

Table 7. Probability of a Rig Operating Day

Month	JUL	AUG	SEP	OCT	NOV
$\hat{p}_s$	0.93	0.79	0.67	0.52	0.59

[7] Because the joint probability information in Table 2 was derived from declustered historical data using a 3 day decorrelation interval, each sample in the simulation that causes a suspension of operations is construed as the onset of an independent weather event. Consequently, one non-operational day is incurred, consistent with the seastate data analysis and the risk mitigation process (rig rotation).

A probability distribution for the number of rig operating days in each month $m\ (m = 1 \dots 5)$ can be estimated using a binomial distribution: $\Pr(Q = q) = \binom{n}{q} \hat{p}_s{}^q (1 - \hat{p}_s)^{n-q}$, where q = number of rig operating days, n = total number of days in the month; $\hat{p}_s$ = estimated probability of a rig operating day. This computation yields a probability distribution of rig operating days for each month as provided in Table 8. Observe that in November, the probabilities are computed only for the first half of the month. This is because the historical availability (based on sea ice) in the second half of November is virtually nil (exactly zero in the observational data used here). Thus, the observed historical seastate conditions are representative of the first half of November only.

Table 8. Probability Distributions of Rig Operating Days per Month (not including availability)

Rig Operating Days	Probability Distributions of Rig Operating Days per Month				
	JUL	AUG	SEP	OCT	NOV
0	2.45E-36	5.37E-22	5.64E-15	1.15E-10	1.73E-06
1	9.93E-34	6.42E-20	3.36E-13	3.91E-09	3.70E-05
2	1.95E-31	3.71E-18	9.67E-12	6.40E-08	3.68E-04
3	2.47E-29	1.38E-16	1.79E-10	6.76E-07	2.27E-03
4	2.26E-27	3.73E-15	2.40E-09	5.16E-06	9.66E-03
5	1.60E-25	7.76E-14	2.48E-08	3.05E-05	3.02E-02
6	9.05E-24	1.30E-12	2.05E-07	1.44E-04	7.16E-02
7	4.23E-22	1.78E-11	1.39E-06	5.62E-04	1.31E-01
8	1.66E-20	2.06E-10	7.96E-06	1.84E-03	1.86E-01
9	5.55E-19	2.03E-09	3.86E-05	5.14E-03	2.06E-01
10	1.60E-17	1.72E-08	1.61E-04	1.23E-02	1.75E-01
11	3.99E-16	1.27E-07	5.81E-04	2.57E-02	1.13E-01
12	8.70E-15	8.15E-07	1.83E-03	4.69E-02	5.36E-02
13	1.66E-13	4.59E-06	5.02E-03	7.48E-02	1.76E-02
14	2.80E-12	2.27E-05	1.21E-02	1.05E-01	3.57E-03
15	4.15E-11	9.93E-05	2.56E-02	1.30E-01	3.39E-04
16	5.43E-10	3.83E-04	4.77E-02	1.42E-01	.
17	6.27E-09	1.30E-03	7.80E-02	1.37E-01	.
18	6.38E-08	3.90E-03	1.12E-01	1.16E-01	.
19	5.71E-07	1.03E-02	1.40E-01	8.68E-02	.
20	4.49E-06	2.38E-02	1.53E-01	5.69E-02	.
21	3.07E-05	4.81E-02	1.45E-01	3.25E-02	.
22	1.83E-04	8.42E-02	1.17E-01	1.61E-02	.
23	9.36E-04	1.27E-01	8.11E-02	6.90E-03	.
24	4.08E-03	1.63E-01	4.69E-02	2.51E-03	.
25	1.50E-02	1.76E-01	2.24E-02	7.68E-04	.
26	4.52E-02	1.57E-01	8.54E-03	1.94E-04	.
27	1.09E-01	1.12E-01	2.51E-03	3.91E-05	.
28	2.05E-01	6.16E-02	5.34E-04	6.11E-06	.
29	2.77E-01	2.45E-02	7.31E-05	6.90E-07	.
30	2.42E-01	6.31E-03	4.84E-06	5.02E-08	.
31	1.02E-01	7.84E-04	.	1.77E-09	.

TOTAL OPERATING DAYS

The final step of the workflow is to combine the preceding outputs regarding availability and rig operating days to produce an estimate of total operating days, or weather window, for a potential season. The final simulation to determine total operating days proceeds as follows, using a sample size of 2,500. Recall that the availability variable was previously sampled for each week and is denoted as ice_w^*. The rig operating days per month is sampled, denoted as q_m^*, for each month using the probability distributions in Table 8. The resulting total operating days in each week and month is defined as: $T_{wm}^* = ice_w^* \times (q_m^*/4)$ for $(w, m) \in \mathcal{J}$ where $\mathcal{J}$ denotes the set of valid (week, month) pairs. The resulting total operating days in each month is defined as $M^* = \sum_{w=1}^{20} T_{wm}^*$, for example, a partial result of 15 samples of this computation of weekly and monthly totals for July is reported in Table 9. The resulting total operating days in each season is defined as $S^* = \sum_{w=1}^{20} \sum_{m=1}^{5} T_{wm}^*$. Statistical properties of the probability distributions for each month and the season are reported in Table 10. The simulated probability distribution of total operating days per season is depicted in Fig. 5.

Table 9. Total Operating Days per Month (July)

	Availability (week #)				Rig Operating Days	Total Operating Days (week #)				Total Operating Days
Sample #	**1**	**2**	**3**	**4**		**1**	**2**	**3**	**4**	
1	1	0	0	0	30	7.50	0.00	0.00	0.00	7.50
2	0	0	0	1	29	0.00	0.00	0.00	7.25	7.25
3	0	1	0	0	30	0.00	7.50	0.00	0.00	7.50
4	0	0	0	1	29	0.00	0.00	0.00	7.25	7.25
5	0	0	0	0	26	0.00	0.00	0.00	0.00	0.00
6	0	0	1	1	28	0.00	0.00	7.00	7.00	14.00
7	0	0	0	0	29	0.00	0.00	0.00	0.00	0.00
8	0	0	1	1	29	0.00	0.00	7.25	7.25	14.50
9	0	0	0	0	30	0.00	0.00	0.00	0.00	0.00
10	0	0	1	0	29	0.00	0.00	7.25	0.00	7.25
11	0	0	0	0	30	0.00	0.00	0.00	0.00	0.00
12	1	0	0	0	27	6.75	0.00	0.00	0.00	6.75
13	0	0	0	1	28	0.00	0.00	0.00	7.00	7.00
14	0	0	0	1	30	0.00	0.00	0.00	7.50	7.50
15	0	0	0	0	30	0.00	0.00	0.00	0.00	0.00

Table 10. Probability Distributions for Total Operating Days (days)

Statistical Property	JUL	AUG	SEP	OCT	NOV	Season
Minimum	0.0	0.0	0.0	1.5	0.0	3.3
P10	0.0	0.0	0.0	11.0	0.0	24.0
P25	0.0	11.5	10.5	14.0	0.0	41.9
Mean	5.4	15.5	15.3	15.2	1.5	52.9
P75	7.5	24.0	21.0	18.0	2.5	66.8
P90	15.0	26.0	23.0	19.0	4.0	74.8
Maximum	31.0	30.0	28.0	25.0	7.5	99.5
Standard Deviation	7.6	8.8	7.6	4.3	1.7	19.1

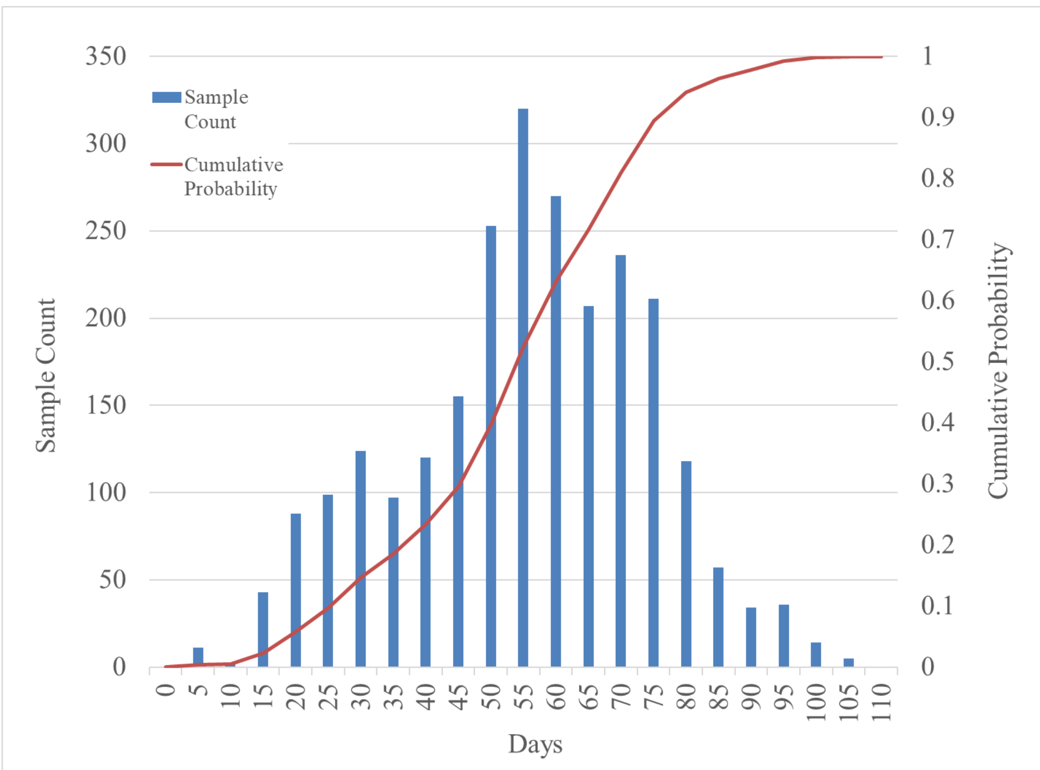

Figure 5. Probability distribution of total operating days per season

In summary, once sea ice availability and vessel-specific operability limits are both taken into account, the average operating season yields only ~53 total operating days—approximately 70% of the days that would appear available from sea-ice availability alone. The distribution is also highly dispersed, with a P10–P90 range of ±25 days. Consequently, any cost and schedule estimate that relies solely on sea ice-based availability or that treats operability as a low-variance (or single-point) value will be materially and systematically over-optimistic.

DRILLING ACTIVITY ANALYSIS

The primary purpose of the weather window estimation is to support probabilistic cost and schedule estimating, with a focus in this analysis on drilling activities. As discussed earlier, Arctic offshore projects incur substantial fixed costs for each operating season. Thus, a primary deliverable of the workflow is to generate probabilistic estimates of the *number of seasons* required to complete a defined scope of work. This information is essential for drilling teams and for numerous other other disciplines—reservoir and production, subsea, facilities, logistics, contracting, and economics—for resource budgeting, financial evaluation, and execution planning.

To demonstrate the approach, we model a four-well drilling campaign. The total uninterrupted duration of the campaign, C^*, is sampled from a uniform distribution, $C^* \sim \mathrm{U}[225{,}375]$ (expected value = 300 days). It is straightforward to respecify the probability distribution to model other definitions of scope, or to investigate the impact of different probability distributions on the estimate (e.g., log-normal). For clarity and simplicity here, we do not include the inefficiencies that arise in drilling activities from interseasonal temporary abandonments and subsequent re-entries—these types of effects can be incorporated in the later phases of detailed cost and schedule estimation if warranted.

Two simulations were completed using 1,000 samples of campaign duration. The first simulation is a partially probabilistic model where the drilling campaign is set at its expected value of 300 days and assessed against 10 sampled seasons of total operating days, S^*, to determine the number of seasons required to complete the sample campaign. The second simulation is fully probabilistic, and a sample of total duration, C^*, is assessed against 10 sampled seasons of total operating days to yield the number of required seasons to complete the campaign. The realizations of drilling campaign duration are assumed to be statistically independent from weather. For comparison, note that the deterministic estimate of the expected number of seasons based on expected values is: $\mathrm{E}[C^*]/\mathrm{E}[S^*] = 300\ \text{days}/52.9\ \text{days per season} = 5.67\ \text{seasons}$ 3 (52.9 days taken from Table 10). The results of both simulations are reported in Table 11.

Table 11. Probability Distribution for Campaign End Date (Season), Four Wells

Season	Partial Probabilistic	Full Probabilistic
1	0	0
2	0	0
3	0	0
4	0.015	0.07
5	0.265	0.268
6	0.47	0.328
7	0.209	0.224
8	0.036	0.082
9	0.005	0.028
10	0	0

The deterministic estimate indicates that the campaign would be completed in season 6, whereas the fully probabilistic model indicates that one-third of campaigns finish in season 7 or later, and more than 10% finish in season 8 or 9. The fully probabilistic model yields thicker tails in both directions and thus demonstrates the incremental value of the fully probabilistic model relative to the deterministic or partially probabilistic model in the context of cost and schedule estimating. The framework presented here is readily extended to alternate definitions of well construction scope and to other types of weather-sensitive activities such as installation of structures, topsides, subsea systems, and pipelines.

CONCLUSIONS

This study specified an integrated probabilistic framework to estimate weather windows for Arctic offshore drilling projects. The simulation generates a site-specific probability distribution of total operating days per season. When coupled with probabilistic drilling or installation activity durations, the workflow generates a probability distribution of the number of seasons required to complete a defined scope of work. The example analysis of a four-well drilling campaign illustrates that deterministic or partially probabilistic models materially underestimate schedule risk relative to a fully probabilistic approach. The principal contribution of this work is a transparent, practical, and novel framework that captures the joint effects of sea ice dynamics, seastate conditions, and operational decision rules. The workflow can be readily extended to all types of well construction campaigns and to other activity types (e.g., subsea installation, pipeline lay). Ultimately, the proposed framework delivers the rigorous quantitative foundation required for accurate and credible cost and schedule estimates in capital-intensive Arctic offshore projects. By explicitly quantifying the large variance and thick tails of seasonal operability, the approach enables more informed economic evaluation, portfolio management, and decision-making—addressing a primary source of uncertainty in Arctic project economics.

REFERENCES

1. BOEM (Bureau of Ocean Energy Management), 2017, "2016a National Assessment of Undiscovered Oil and Gas Resources of the U.S. Outer Continental Shelf," US Department of the Interior, Bureau of Ocean Energy Management, OCS Report BOEM 2017-085.
2. USGS (U.S. Geological Survey), 2008, "Circum-Arctic Resource Appraisal: Estimates of Undiscovered Oil and Gas North of the Arctic Circle, USGS Fact Sheet 2008-3049," U.S. Department of the Interior, Washington D.C., USA.
3. Maes, M.A., Sinclair, J., and Lewis, D.B., 2005, "Risk Analysis of Running a Deep-Water Production Test from a Dynamically Positioned Vessel in the North Atlantic," *J. Offshore Mech. Arct. Eng*., **127**(1), pp. 52–58.
4. Li, L., Guachamin Acero, W., Gao, Z., and Moan, T., 2016, "Assessment of Allowable Sea States During Installation of Offshore Wind Turbine Monopiles with Shallow Penetration in the Seabed," *J. Offshore Mech. Arct. Eng*., **138**(4): 041902.
5. Rahman, M.S., Khan, F., Shaikh, A., Ahmed, S., and Imtiaz, S., 2019, "Development of risk model for marine logistics support to offshore oil and gas operations in remote and harsh environments," *Ocean Engineering*, **174**, pp. 125-134.
6. Towe, R., Zanini, E., Randell, D., Feld, G., and Jonathan, P., 2021, "Efficient estimation of distributional properties of extreme seas from a hierarchical description applied to calculation of un-manning and other weather-related operational windows," *Ocean Engineering*, **238**: 109642.
7. Heo, T., Liu, D.P., and Manuel, L., 2023, "Weather Window Analysis in Operations and Maintenance Policies for Offshore Floating Multi-Purpose Platforms," *J. Offshore Mech. Arct. Eng*., **145**(4): 041701.
8. Walker, R.T., van Nieuwkoop-McCall, J., Johanning, L., and Parkinson, R.J., 2013, "Calculating weather windows: Application to transit, installation and the implications on deployment success," *Ocean Engineering*, **68**, pp. 88-101.
9. Yang, Z., Lin, Y., and Dong, S., 2022, "Weather window and efficiency assessment of offshore wind power construction in China adjacent seas using the calibrated SWAN model," *Ocean Engineering*, **259**: 111933.
10. Eubank, S..B., and White, James M., 1957, "Use of the Monte Carlo Technique for the Engineering Economist," *Engineering Economist*, **3**(2), pp. 1-17.
11. Cardello, R.A., Kellett, J.W., and Lukk, G.G., 1963, "Determining the Proper Size of Manufacturing Projects," *Engineering Economist*, **9**(1), pp. 1-25.
12. White, James McD., 1968, "The Optimal Design of a Refinery," *Engineering Economist*, **13**(4): 199-210.
13. Klausner, Robert F., 1969, "The Evaluation of Risk in Marine Capital Investments," *Engineering Economist*, **14**(4): pp. 183-214.
14. Farr, John V., Faber, Isaac J., Ganguly, Anirban, Martin, W. Andy, and Larson, Steven L., 2016, "Simulation-based costing for early phase life cycle cost analysis: Example application to an environmental remediation project," *Engineering Economist*, **61**(3), pp. 207-222.
15. Leheta, Heba Wael, Elhanafi, Ahmed Shawki, and Badran, Sherif Farouk, 2016, "Reliability Analysis of Novel Stiffened Panels Using Monte Carlo Simulation," *Ships and Offshore Structures*, **12**(5), pp. 640-652.
16. de Werk, M., Ozdemir, B., Ragoub, B., Dunbrack, T., and Kumral, M., 2016, "Cost Analysis of Material Handling Systems in Open Pit Mining: Case Study on an Iron Ore Prefeasibility Study," *Engineering Economist*, **62**(4), pp. 369-386.
17. Zoller, S.L., Graulier, J.-R., and Paterson, A.W., 2003, "How Probabilistic Methods Were Used to Generate Accurate Campaign Costs for Enterprise's Bijupirá & Salema Development," Paper SPE 79902 presented at the *SPE/IADC Drilling Conference*, Amsterdam, Netherlands. https://doi.org/10.2118/79902-MS.

18. Williamson, H.S., Sawaryn, S.J., and Morrison, J.W., 2004, “Some Pitfalls in Well Forecasting,” Paper SPE 89984 presented at the *SPE Annual Technical Conference and Exhibition*, Houston, TX, USA. https://doi.org/10.2118/89984-MS
19. Akins, W.M., Abell, M.P., and Diggins, E.M., 2005, “Enhancing Drilling Risk and Performance Management Through the Use of Probabilistic Time and Cost Estimating,” Paper SPE 92340 presented at the *SPE/IADC Drilling Conference*, Amsterdam, Netherlands. https://doi.org/10.2118/92340-MS.
20. Hariharan, P.R., Judge, R.A., and Nguyen, D.M., 2006, “The Use of Probabilistic Analysis for Estimating Drilling Time and Costs While Evaluating Economic Benefits of New Technologies,” Paper SPE 98695 presented at the *IADC/SPE Drilling Conference*, Miami, Florida, USA. https://doi.org/10.2118/98695-MS
21. Kaiser, M.J. and Pulsipher, A.G., 2007, “Generalized Functional Models for Drilling Cost Estimation,” *SPE Drilling and Completions*, **22**(2), pp. 67–73.
22. Adams, A.J., Gibson, C., and Smith, R., 2009, “Probabilistic Well Time Estimation Revisited,” Paper SPE 119287 presented at the *SPE/IADC Drilling Conference and Exhibition*, Amsterdam, Netherlands. https://doi.org/10.2118/119287-MS.
23. Jablonowski, C., Ettehad, A., Ogunyomi, B., and Srour, I., 2011, “Integrating Learning Curves in Probabilistic Well Construction Estimates,” *SPE Drilling and Completions*, **26**(1), pp. 133-138.
24. NRC (National Research Council), 2014, “Responding to Oil Spills in the U.S. Arctic Marine Environment,” The National Academies Press, Washington D.C., USA.
25. Pan, K., Song, J., Fu, Y., Guo, J., Bai, G., and Cai, Y., 2025, “Spatiotemporal variability of sea ice and its meteorological drivers in Liaodong Bay, China (2014–2024),” *Ocean Engineering*, **336**: 121770.
26. Steele, M., Bliss, A. C., Peng, G., Meier, W. N. and Dickinson, S., 2019, “Arctic Sea Ice Seasonal Change and Melt/Freeze Climate Indicators from Satellite Data (NSIDC-0747, Version 1),” Boulder, Colorado, USA.
27. Bliss, A.C., Steele, M., Peng, G., Meier, W.N., and Dickinson, S., 2019, “Regional variability of Arctic sea ice seasonal change climate indicators from a passive microwave climate data record,” *Environ. Res. Lett*., **14**: 045003.
28. Peng, G., Steele, M., Bliss, A.C., Meier, W.N., and Dickinson, S., 2018, “Temporal Means and Variability of Arctic Sea Ice Melt and Freeze Season Climate Indicators Using a Satellite Climate Data Record,” *Remote Sens*., **10**(9): 1328.
29. Eik, K.J., 2008, “Review of Experiences within Ice and Iceberg Management,” The Journal of Navigation, **61**(4), pp. 557-572.
30. Eik, K.J., 2010, “Ice Management in Arctic Offshore Operations and Field Development,” *Ph.D. Dissertation*, Norwegian University of Science and Technology, Trondheim, Norway.
31. Teigen, S.H., Eik, K.J., Bernard-Grand’Maison, C., Hall, R., 2023, “Ice risk management for drilling operations in the Southern Barents Sea,” *27th International Conference on Port and Ocean Engineering under Arctic Conditions*, Glasgow, United Kingdom.
32. Meier, W.N., Petty, A., Hendricks, S., Bliss, A., Kaleschke, L., Divine, D., Farrell, S., Gerland, S., Perovich, D., Ricker, R., Tian-Kunze, X., and Webster, M., 2024, “Arctic Report Card: Update for 2024,” NOAA, Silver Spring, MD, USA. DOI: 10.25923/aksk-7p66
33. Eayrs, C., Holland, D., Francis, D., Wagner, T., Kumar, R. and Li, X., 2019, “Understanding the Seasonal Cycle of Antarctic Sea Ice Extent in the Context of Longer-Term Variability,” *Reviews of Geophysics*, **57**(3), pp. 1037-1064.
34. Msadek, R., Vecchi, G.A., Winton, M., Gudgel, R.G. 2014. Importance of initial conditions in seasonal predictions of Arctic sea ice extent. *Geophysical Research Letters*, **41**(14).
35. Chen, D., and Yuan, X., 2004. “A Markov model for seasonal forecast of Antarctic sea ice,” *J. Climate*, **17**, pp. 3156–3168.
36. Yuan, X., Chen, D.M., Li, C., Wang, L., and Wang, W., 2016, “Arctic Sea Ice Seasonal Prediction by a Linear Markov Model,” *Journal of Climate*, **29**(22), pp. 8151-8173.
37. Wang, Y., Yuan, X., Bi, H., Bushuk, M., Liang, Y., Li, C., and Huang, H., 2022, “Reassessing seasonal sea ice predictability of the Pacific-Arctic sector using a Markov model,” *The Cryosphere*, **16**, pp. 1141–1156.

38. API (American Petroleum Institute), 2014, “Derivation of Metocean Design and Operating Conditions, ISO 19901-1:2005 (Modified), Petroleum and natural gas industries - Specific requirements for offshore structures - Part 1: Metocean design and operating considerations, First Edition,” American Petroleum Institute, Washington D.C., USA.
39. Guedes Soares, C., and Carvalho, A.N., 2003, “Probability Distributions of Wave Heights and Periods in Measured Combined Sea-States from the Portuguese Coast,” *J. Offshore Mech. Arct. Eng*., **125**(3), pp. 198-204.
40. Fouques, S., Myrhaug, D., and Nielsen, F.G., 2004, “Seasonal Modeling of Multivariate Distributions of Metocean Parameters with Application to Marine Operations,” *J. Offshore Mech. Arct. Eng*., **126**(3), pp. 202-212.
41. Bitner-Gregersen, E.M., Ewans, K.C., and Johnson, M.C., 2014, “Some uncertainties associated with wind and wave description and their importance for engineering applications,” *Ocean Engineering*, **86**, pp. 11-25.
42. Martins Campos, R., D’Agostini, A., Reis Leite França, B., Machado Cruz, L., and Guedes Soares, C., 2021, “Extreme Wind and Wave Predictability from Operational Forecasts at the Drake Passage,” *J. Offshore Mech. Arct. Eng*., **143**(2): 021703.
43. Liao, Z., Huang, W., Dong, S., and Li, H., 2022, “Modelling trivariate distribution of directional ocean data in the Barents Sea seasonal ice zone,” *Ocean Engineering*, **260**: 111745.
44. Yang, Z., Yang, Y., Xing, A., and Qin, J., 2025, “A novel optimization framework of joint evolving extreme-aimed probabilistic modeling for wind speed and significant wave height,” *Ocean Engineering*, **339**: 122101.
45. Thomson, J., Rogers, W.E., 2014, “Swell and Sea in the Emerging Arctic Ocean,” *Geophysical Research Letters,* **41**, pp. 1-5.
46. Donley, M.G., and Spanos, P.D., 1991, “Stochastic Response of a Tension Leg Platform to Viscous Drift Forces,” *J. Offshore Mech. Arct. Eng*., **113**(2), pp. 148–155.
47. Winterstein, S.R., and Torhaug, R., 1996, “Extreme Jack-Up Response: Simulation and Nonlinear Analysis Methods,” *J. Offshore Mech. Arct. Eng*., **118**(2), pp. 103–108.
48. Winterstein, S.R., Torhaug, R., and Kumar, S., 1998, “Design Seastates for Extreme Response of Jackup Structures,” *J. Offshore Mech. Arct. Eng*., **120**(2), pp. 103–108.
49. Cassidy, M.J., Houlsby, G.T., and Eatock Taylor, R., 2003, “Probabilistic Models Applicable to the Short-Term Extreme Response Analysis of Jack-Up Platforms,” *J. Offshore Mech. Arct. Eng*., **125**(4), pp. 249–263.
50. Karimirad, M., and Moan, T., 2011, “Extreme Dynamic Structural Response Analysis of Catenary Moored Spar Wind Turbine in Harsh Environmental Conditions,” *J. Offshore Mech. Arct. Eng*., **133**(4): 041103.
51. Ahmad, S., and Datta, T.K., 1990, “Probabilistic Pseudo-Static Analysis of Risers,” *J. Offshore Mech. Arct. Eng*., **112**(1), pp. 58–64.
52. Sheehan, J.M., Grealish, F.W., Harte, A.M., and Smith, R.J., 2006, “Characterizing the Wave Environment in the Fatigue Analysis of Flexible Risers,” *J. Offshore Mech. Arct. Eng*., **128**(2), pp. 108–118.
53. Ward, P., Rimmer, A., and Howells, H., 2013, “Evaluation of Wellhead Fatigue Using In-Service Structural Monitoring Data,” Paper OTC 23981 presented at the *Offshore Technology Conference*, Houston, TX, USA.
54. McNeill, S., Agarwal, P., Kluk, D., Bhalla, K., Young, R., Burman, S., Liapis, S., Jain, S., Jhingran, V., Hodges, S., and Denison, E., 2014, “Subsea Wellhead and Riser Fatigue Monitoring in a Strong Surface and Submerged Current Environment,” Paper OTC-25403-MS presented at the *Offshore Technology Conference*, Houston, TX, USA.